Proceedings
of the 4th International Modelica Conference,
Hamburg, March 7-8, 2005,
Gerhard Schmitz (editor)

W. Casas, K. Prölß , G. Schmitz
TUHH, Germany
Modeling of Desiccant Assisted Air Conditioning Systems
pp. 487-496

Paper presented at the 4th International Modelica Conference, March 7-8, 2005,
Hamburg University of Technology, Hamburg-Harburg, Germany,
organized by The Modelica Association and the Department of Thermodynamics, Hamburg University of Technology

All papers of this conference can be downloaded from
http://www.Modelica.org/events/Conference2005/

Modeling of Desiccant Assisted Air Conditioning Systems

Wilson Casas*, Katrin Proelss and Gerhard Schmitz
Technische Universität Hamburg-Harburg
Denickestr. 17, 21075 Hamburg, Germany

Abstract

In desiccant air conditioning systems, moist air is dehumidified by means of a desiccant wheel. Water vapour is absorbed by desiccant material as humid air passes through the wheel. Using this technology, considerable energy savings can be obtained compared to conventional air conditioning systems. To evaluate the performance of the desiccant assisted air conditioning process, a model library has been developed. In this paper, control volume models for humid air and desiccant material are implemented and finally the operation of the desiccant wheel is simulated. Comparison of the dynamic and steady state results to open literature, manufacturer data as well as experimental result is used to validate the model.

Keywords: air conditioning; desiccant wheel; sorption; rotating heat exchanger, modelica

1 Introduction

In a desiccant assisted system, moist air is first dehumidified using a desiccant wheel, see figure 1. The wheel consists of a honeycomb structure, which is coated with desiccant materials such as silica gel or lithium chloride. Water vapour is absorbed by the desiccant material as humid air passes through the wheel. The moisture is released when the desiccant is regenerated by heating. For regenerating the desiccant wheel, heat input at relatively low temperatures (e.g. 60-70°C) is required, depending on the desiccant material. Using desiccant technology, the cooling demand can be reduced to 30% of that of a conventional system [2]. The energy demand for air conditioning is thus shifted from electrical to thermal energy, primary energy consumption is reduced as well and waste heat can be used.

The performance of the desiccant wheel depends on several parameters, like ambient air condition (temperature and humidity), regeneration air, volume flow rates and rotation speed. Other wheel specific parameters are geometry structure and sorption properties of the material.

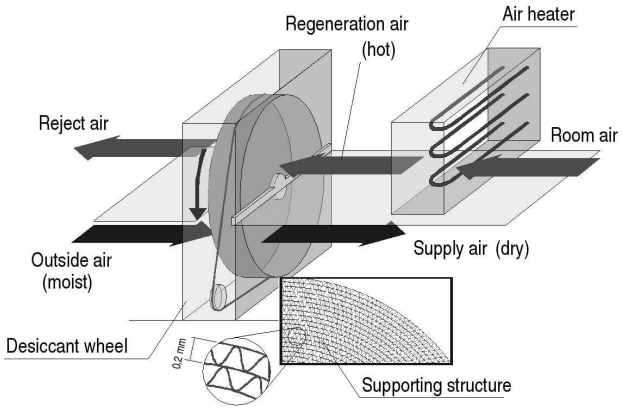

Figure 1: Desiccant wheel for air conditioning systems

In order to predict heat and moisture transfer in the desiccant wheel, conservation equations for energy and mass need to be postulated. Convective heat and mass transfer are described by lumped coefficients, whereby heat and moisture transfer are coupled by the equilibrium condition of the desiccant material, the so called sorption isotherm. Conservation equations, heat and mass transfer, the sorption isotherm as well as thermodynamic state equations for air and desiccant material result in a complex, non-linear, differential algebraic system of equations (DAE).

Several solutions for such DAEs have been provided in different works. [6] introduces the concept of characteristic potentials, whereby the DAE is rewritten based on these new independant variables. Using heat and mass transfer analogy, a numerical solution for the DAE can be provided. Other authors solved the DAE by linearization and Laplace-Transformation [7], using a finite difference method [14], or finite volume method with a Gauss-Seidel iteration algorithm [13].

*email: casas@tu-harburg.de, Tel:+40 4042878 3079

As this short literature review shows, providing a solution for the combined heat and mass transfer problem in the desiccant wheel requires expert knowledge of the applied numerical methods as well as good programming skills. In addition, governing equations have to be rewritten in a very abstract form (for example using dimensionless variables).
A limitation of most of the methods available in the open literature is, that they can not be used for desiccant materials with discontinuities in their sorption isotherms (e.g. lithium chloride), unless the solver algorithm is extended or rewritten [9]. Hence, in case of lithium chloride as desiccant material, numerical solution methods based on heat and mass transfer analogy mentioned above can not be applied.
In this work Modelica/Dymola was used to overcome these limitations and to provide a component oriented modeling approach which offers a high level of flexibility with respect to boundary settings.

2 Physical Model

In air conditioning systems, or thermodynamics systems in general, a working fluid (e.g. air, water) flows through several components (e.g. ventilators, heating or cooling coils). Components can be modeled by algebraic equations or by partial differential equations. In this case, a distributed approach with higher discretization may be necessary. A control volume for humid air is therefore needed.

2.1 Humid air

The model for humid air described here is based on following assumptions:

(1) Humid air is an ideal mixture, Dalton's Law of Partial Pressures is valid.

(2) Air flow is incompressible.

(3) Constant specific heat capacities for dry air, water vapour and liquid water.

(4) Heat conduction in flow direction is neglected.

Balance and state equations will be postulated for a control volume according to figure 2. The control volume model is assumed to be connected to other models, whereby heat and humidity or air can be exchanged.
Specific values (e.g. enthalpy h, internal energy u) used in the equations below are defined with respect

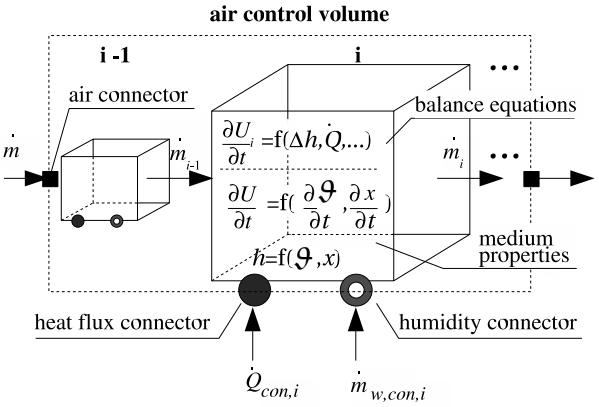

Figure 2: Air control volume

to dry air mass. Water content or absolute humidity of air x is defined as the ratio of water to dry air mass,

$$x_i = \frac{M_{w,i}}{M_i} \tag{1}$$

The energy balance for an i control volume can be written as

$$\begin{aligned} \frac{\partial U_i}{\partial t} &= \dot{Q}_{con,i} + \dot{m}_{i-1} \cdot h_{i-1} - \dot{m}_i \cdot h_i \\ &\quad + \dot{m}_{w,con,i} \cdot h_{w,con,i} \end{aligned} \tag{2}$$

$\dot{Q}_{con,i}$ is the sensible heat flux and $h_{w,con,i}$ denotes the enthalpy of the exchanged moisture. Consequently the term $\dot{m}_{w,con,i} \cdot h_{w,con,i}$ equals the latent heat flux. The dry air mass balance is given by the simple equation

$$\frac{\partial M_i}{\partial t} = \dot{m}_i - \dot{m}_{i-1} \quad . \tag{3}$$

Water balance results in the relationship

$$\frac{\partial M_{w,i}}{\partial t} = \frac{\partial x_i}{\partial t} \cdot M_i = \dot{m}_{w,con,i} + \dot{m}_{i-1} \cdot x_{i-1} - \dot{m}_i \cdot x_i \quad . \tag{4}$$

The dynamic caloric state equation can be obtained from the ideal gas equations,

$$\frac{\partial u_i}{\partial t} = \frac{\partial h_i}{\partial t} - R \cdot \frac{\partial \vartheta_i}{\partial t} \quad . \tag{5}$$

Thereby, enthalpy of humid air is

$$h_i = c_{p,a} \cdot \vartheta_i + x_i \cdot (c_{p,wv} \cdot \vartheta_i + \Delta h_V) \tag{6}$$

and its derivative

$$\begin{aligned} \frac{\partial h_i}{\partial t} &= c_{p,a} \cdot \frac{\partial \vartheta_i}{\partial t} + (c_{p,wv} \cdot \vartheta_i + \Delta h_V) \\ &\quad \cdot \frac{\partial x_i}{\partial t} + x_i \cdot c_{p,wv} \cdot \frac{\partial \vartheta_i}{\partial t} \quad . \end{aligned} \tag{7}$$

From this follows

$$\frac{\partial u_i}{\partial t} = (c_{p,a} - R_a + x_i \cdot (c_{p,wv} - R_w)) \cdot \frac{\partial \vartheta_i}{\partial t} + (c_{p,wv} \cdot \vartheta_i + \Delta h_V) \cdot \frac{\partial x_i}{\partial t} \quad . \tag{8}$$

Dynamic equations for air states may not be needed for every final component model. Hence, it makes sence to implement steady equations

$$\frac{\partial u_i}{\partial t} = 0 \quad \text{and} \quad \frac{\partial x_i}{\partial t} = 0 \tag{9}$$

to be used instead. With an appropriate parameter, the developer may be able to decide if dynamic or steady state equations are to be used.

2.2 Desiccant material and supporting structure

First, a control volume for the supporting structure according to figure 3 is defined. Since the wheel has to be discretized in axial and eventually also in tangential direction, it is advantageous to choose a "pie piece" of the wheel. The control volume will be connected later to the humid air model using the heat flux and moisture connectors. Following assumptions are made:

(1) The homogeneous, uniform wheel consists of supporting material (e.g. cellulose) and desiccant material (mass fraction χ) both with constant specific heat capacities c_r and c_s.

(2) Axial heat conduction is neglected.

(3) Humidity transport and diffusion in the wheel is neglected.

(4) Heat and mass transfer between air and matrix can be described by lumped transfer coefficients.

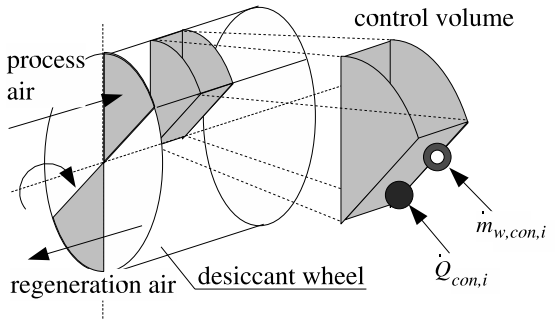

Figure 3: Convective heat and moisture transfer

The mass of the matrix material in a control volume V follows from

$$M_i = V_i \cdot \rho_r \quad , \tag{10}$$

where ρ_r is the density of the supporting structure.
The humidity ratio in the desiccant material is defined as

$$q_i = \frac{M_{w,i}}{\chi \cdot M_i} \quad . \tag{11}$$

The change of water in control volume can be calculated from

$$\frac{\partial M_{w,i}}{\partial t} = M_i \cdot \chi \cdot \frac{\partial q_i}{\partial t} = \dot{m}_{w,con,i} \quad , \tag{12}$$

whereby $\dot{m}_{w,con,i}$ equals the sorbed or desorbed water. The energy balance results in

$$\frac{\partial U_i}{\partial t} = \dot{Q}_{con,i} + \dot{m}_{w,con,i} \cdot h_{w,con,i} \quad . \tag{13}$$

As for the air side, $\dot{Q}_{con,i}$ is the sensible heat, $\dot{m}_{w,con,i} \cdot h_{w,con,i}$ the latent heat transferred with the moisture. Enthalpy of sorbed water vapour comprises heat of sorption, which consists of heat of vaporization and binding enthalpy,

$$\begin{aligned} h_{w,con,i} &= \Delta h_{S,i} + c_{p,wv} \cdot \vartheta_{a,i} \\ &= \Delta h_{B,i} + \Delta h_V + c_{p,wv} \cdot \vartheta_{a,i} \quad . \end{aligned} \tag{14}$$

Binding enthalpy $\Delta h_{B,i}$ depends on the desiccant material properties and is supposed to be known from experimental data.
From the enthalpy of wet material

$$h_i = (c_r + c_s \cdot \chi + \chi \cdot q_i \cdot c_w) \cdot \vartheta_i \tag{15}$$

follows the dynamic state equation

$$\begin{aligned} \frac{\partial u_i}{\partial t} &= (c_r + c_s \cdot \chi + \chi \cdot q_i \cdot c_w) \frac{\partial \vartheta_i}{\partial t} \\ &+ \chi \cdot q_i \cdot c_w \cdot \vartheta_i \cdot \frac{\partial q_i}{\partial t} \quad . \end{aligned} \tag{16}$$

The convective heat transfer between air and desiccant material (see figure 4) can be described using Newton's Law of Cooling,

$$\dot{Q}_{con,i} = \alpha_i \cdot A_{e,i} \cdot (\vartheta_{a,i} - \vartheta_i) \tag{17}$$

$A_{e,i}$ denotes the effective heat transfer area, $\vartheta_{a,i}$ is the fluid temperature and α_i the local heat transfer coefficient. The effective heat transfer area can be written as the ratio of Volume to specific surface

$$A_{e,i} = \frac{V}{\omega} \quad , \tag{18}$$

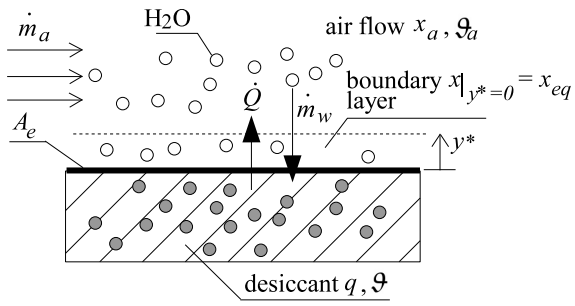

Figure 4: Convective heat and moisture transfer

Table 1: Geometry data for desiccant wheel

$2b$	2,0 mm
$2a$	3,4 mm
c	0,125 mm
U	8,84 mm
A	3,4 mm^2
D_h	1,539 mm
ω	2600 m^2/m^3
ρ_r	129,5 kg/m^3

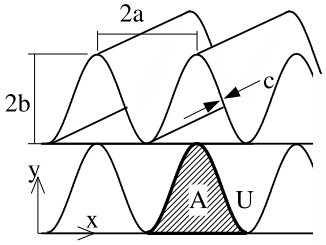

whereby specific surface can be calculated from rotor geometry, refer to table 1.

The *Nusselt*-Number $Nu = \alpha \cdot D_h/\lambda$ and thus also the heat transfer coefficient for laminar flow in sinusoidal ducts can be obtained from numerical work [8, 12, 1, 11].

In analogy to (17), convective mass transfer could be described by

$$\dot{m}_{w,con,i} = \beta_i \cdot \rho_{a,i} \cdot A_{e,i} \cdot (x_{a,i} - x|_{y^*=0}) \quad . \qquad (19)$$

β_i denotes thereby the mass transfer coefficient and $x|_{y^*=0}$ is the moisture content of the boundary layer at the surface of the desiccant material. Hence concentration difference $(x_{a,i} - x|_{y^*=0})$ is the driving force for convective moisture transfer. It has to be assumed, that the boundary layer is in equilibrium with the wall with respect to temperature and moisture content, for instance water content of the boundary layer $x|_{y^*=0}$ equals $x_{eq} := f(q, \vartheta_w)$, namely the water content of air at equilibrium with desiccant of water load q and temperature of matrix ϑ.

Sorption equilibrium is given by the sorption isotherm

$$q_{eq} = q(p_{wv}, \vartheta) \qquad (20)$$

describing the equilibrium moisture content of desiccant for a constant temperature depending on vapour partial pressure. The function $q(p_{wv}, \vartheta)$ is usually given as a correlation of measurement data. Another equivalent formulation is

$$p_{eq} = p(q, \vartheta) \qquad (21)$$

denoting the equilibrium partial pressure for a known moisture content and temperature.

For most solid desiccants (e.g. silicagel), the sorption isotherm is continuous. For lithium chloride, depending on water content, sorption isotherm slope changes discontinuously due to phase changes of the system (LiCl hydrate formation). As figure 5 shows, for the interesting temperature range of $20 - 90°C$, the LiCl-water system can consist of dilute solution, saturated solution with monohydrates or anhydrous LiCl and monohydrates. Figure 6 shows sorption isotherms from experimental data [5] and the developed correlation used in this work, as well as other correlations [3].

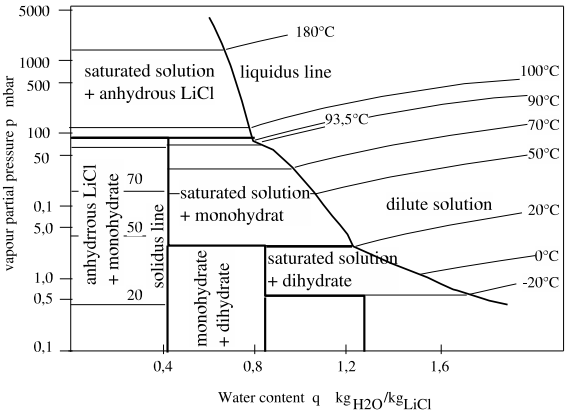

Figure 5: Phase diagram for the system LiCl-water (based on [10])

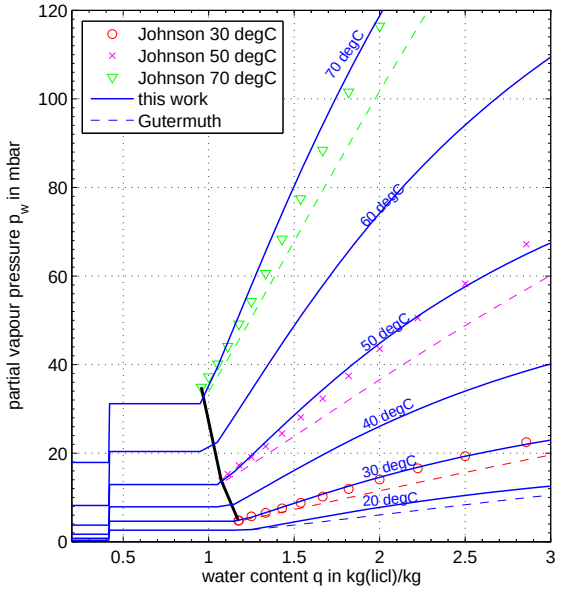

Figure 6: Sorption isotherms for the system LiCl-water

It should be noticed, that for implementation in Modelica, appropiate crossing functions should be used to avoid numerical instabilities during simulation and to reduce computation time.
If the sorption equilibrium equation (21) is known, x_{eq} in (19) follows to

$$x_{eq,i} = \frac{R_a}{R_w} \cdot \frac{p_{eq,i}(q,\vartheta_i)}{(p - p_{eq,i}(q,\vartheta_i))} \tag{22}$$

To determine the convective mass transfer coefficient in (19), the *Lewis* number $Le = a/D_{12}$ may be used to relate the two convective transfer coefficients [4]

$$\frac{\alpha}{\beta} = \frac{\lambda}{D_{12} \cdot Le^n} = \rho \cdot c_p \cdot Le^{(1-n)} \quad . \tag{23}$$

It has to be pointed out, that the relationship given above can only be used, if convective mass transfer at the surface dominates the overall mass transfer resistance. Other moisture transport mechanisms in the material (e.g. pore diffusion) are thus neglected.

3 Modelica implementation

The humid air and desiccant models were implemented in a Modelica library. The base model of the desiccant wheel `RotPair` is built up from two pairs of each one air and desiccant wall model instances, see figure 7. Each air and desiccant wall component is divided into n elements (control volumes). The two model pairs represent two opposites "pie pieces" of the desiccant wheel (see figure 3), so one model pair is in the regeneration and the other in the process air stream. After half a revolution, the boundary conditions (air inlet) changes, since the pie piece goes from process to regeneration side. Therefore, auxiliary models have to be used and outer connectors can not be joined directly to air models. In addition, during regeneration, the first element ($i = 1$) of the desiccant wall model is connected to the last element of the corresponding air model ($i = n$). Boolean signal connectors are used to change the connection order in the desiccant wall model according to the angular position of the pie piece in the wheel.
Higher discretisation in tangential direction (more "pie pieces") can be used, but computation time increases drastically. In addition to increased number of equations in the system, more state events are generated during simulation each time boundary conditions change. Discretisation in tangential direction makes hence only sence, if inlet conditions change with time

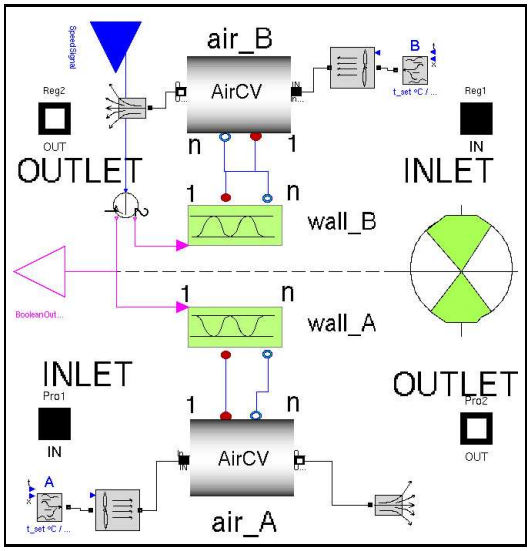

Figure 7: `RotPair` Desiccant wheel base model (diagramm layer)

rapidly. In that case, outlet conditions have to be computed as a mean value from m pie elements. If only one pie element is simulated, and inlet conditions are constant, air outlet conditions result as mean value for half a revolution and is therefore integrated over time, e.g. for temperature

$$\bar{\vartheta}_{out} = \frac{1}{\Delta t} \int_t^{t+\Delta t} \vartheta \, dt \tag{24}$$

Figure 8 plots the temperature of both pie piece control volumes at the process air outlet side and the calculated time mean value according to equation above. Concerning axial discretisation, best compromise is obtained with $n = 10 \ldots 15$ for a wheel width of 250 mm.

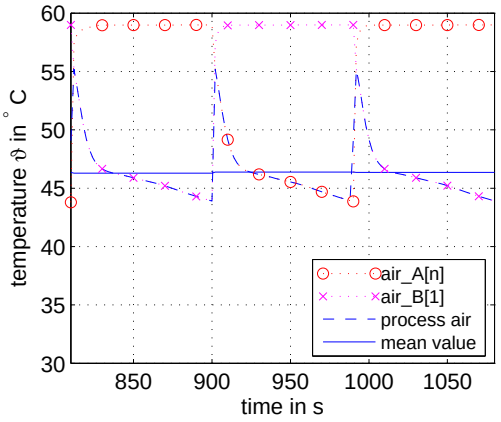

Figure 8: Mean value computation for rotating speed 1/3 rpm ($\Delta t = 90$ s)

Figure 9 shows the structure of the `RotPair` model.

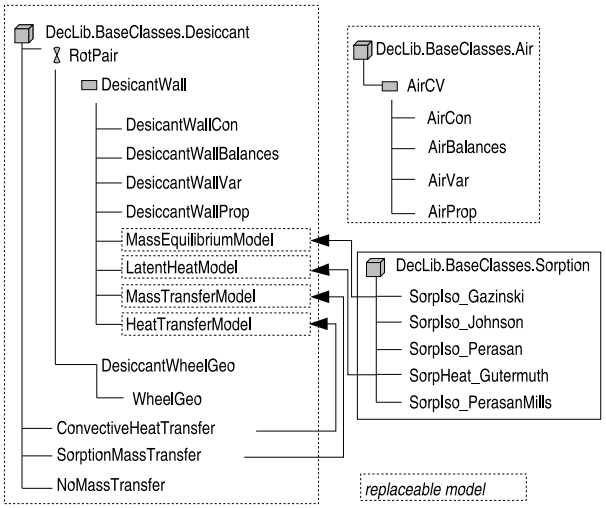

Figure 9: Structure of the model

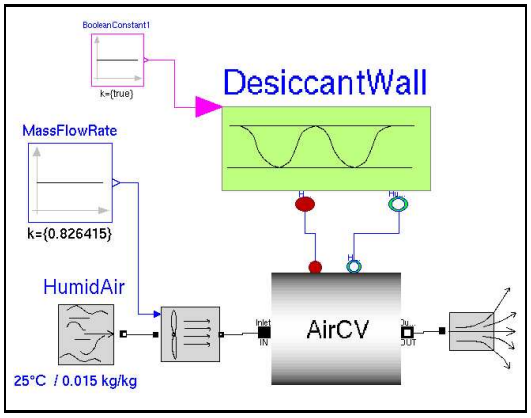

Figure 10: Test model for dynamic simulation

The `DesiccantWall` model consists of several classes containing balance equations and material properties. In order to use the same model with other desiccant materials (e.g. Silicagel) or for simulation of rotary heat exchangers (no mass transfer at all), some classes are replaceable. For instance, the `MassEquilibriumModel` containing the description of the sorption isotherm can easily be exchanged, as well as the latent (sorption) heat model.

4 Simulation results

In this section, first dynamic simulation results will be shown and compared to open literature. Subsequently, results from steady state simulation will be discussed and a total system simulation will be presented.

4.1 Dynamic simulation

The Modelica model described in this paper was used to simulate the dynamic behaviour of a rotary LiCl dehumidifier, see figure 10. The matrix is assumed to be at a regenerated state with uniform temperature $\vartheta_{init} = 75°C$ and water load of $q_{init} = 0.3$ kg/kg. The air flows through the matrix with an inlet temperature $\vartheta_{a,in} = 25°C$ and humidity $x_{a,in} = 15$ g/kg. Initial conditions and other parameters chosen here correspond to those used in [9], so simulation results can be compared.

The temperature and water content profile of the matrix with respect to the axial coordinate are shown in figure 11a,b. Each curve corresponds to one time snapshot. Figure 11c,d shows the temperature and moisture content of outlet air during the process.

At the beginning of the process, the hot matrix is cooled down very fast, since sensible heat exchange due to high temperature differences between matrix and air dominates. It can be seen that outlet temperature of air rises very quickly (inlet 25°C, outlet 73°C). But after a few seconds, the temperature in the matrix remains at 56°C. At this temperature, a phase change in LiCl-water system from hydrate to saturated solution occurs. Equilibrium condition changes and sorption rate decreases, resulting in a rising outlet moisture content of the air. The next phase change from saturated solution to unsaturated solution occurs at 46°C. During this process, outlet air states stay nearly constant. When only unsaturated solution remains, the sorption rate drops and air outlet states approach the inlet conditions rapidly.

Simulation results show good agreement with theoretical simulations in [9]. Differences in temperature and moisture content appear, which could be due to different equations for the description of sorption isotherms between [9] and the present work.

4.2 Steady state simulation

Figure 12 shows the air outlet moisture content of the air for a LiCl rotary dehumidifier (diameter 895 mm, $\dot{V} = 2300$ m^3/h) at constant process air inlet temperature $\vartheta_{a,in} = 32°C$ and rotation speed 1/3 rpm depending on inlet humidity and regeneration temperature. For comparison, manufacturer data is plotted in dashed lines.

As can be seen, outlet humidity decreases at higher regeneration temperatures, but there is a deviation of approximately 0,5 g/kg between simulation and manufacturer data. Besides of that, outlet humidity according to manufacturer appears to decrease linearly with respect to regeneration temperature, whereas sim-

a)

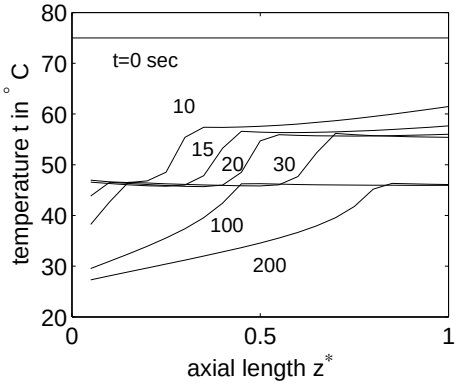

b)

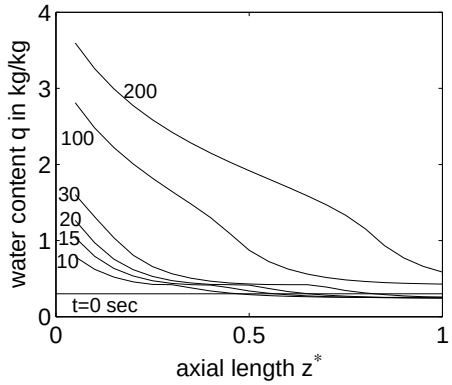

c)

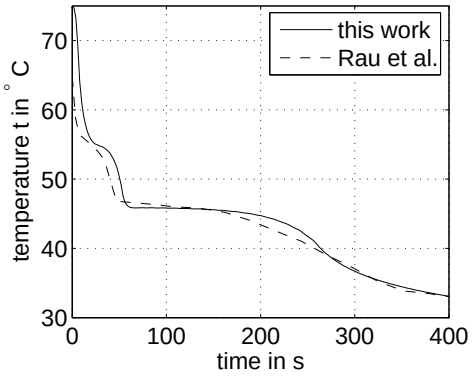

d)

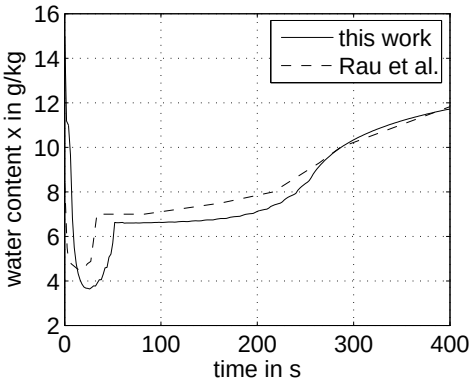

Figure 11: Dynamic simulation results: a) matrix temperature and b) water content, c) air outlet temperature and d) water content

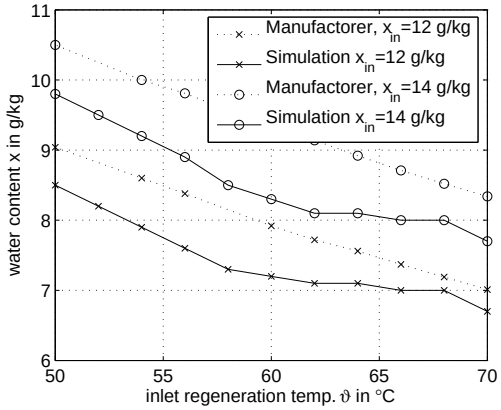

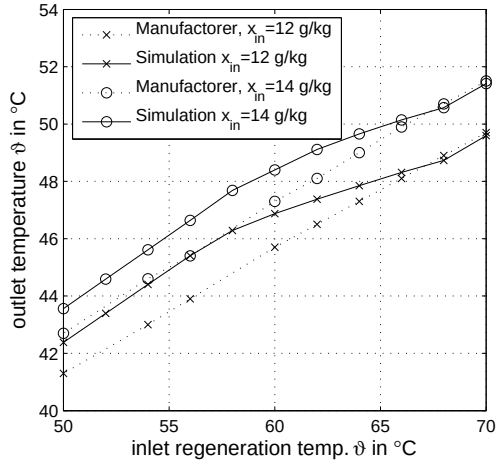

Figure 12: Air outlet water content and temperature for different regeneration temperatures, comparison between simulation and manufacturer data

ulated humidity approaches a limiting value at $\vartheta_{a,reg} = 68°C$ and decreases again for higher temperatures. This behaviour is in full agreement with the sorption isotherm: for temperatures at around $60 \ldots 65°C$ LiCl saturated solution forms at the regeneration side. Lower matrix water load does not result in higher sorption potential according to sorption isotherm. Only if water load is reduced under a certain value, anyhdrous LiCl can form and sorption potential is higher. Although there is a limit for outlet humidity – if regeneration temperature is high enough, so that the whole matrix can be dryed ($q \to 0$), increasing regeneration temperature does not affect outlet humidity. This behaviour is in agreement with simulation results for higher temperatures (e.g. 80°C, not shown in figure 12). Manufacturer data seems not to comply with this limit and there is no data available for higher regeneration temperatures.

In terms of outlet temperature, simulation results show good agreement with manufacturer data. Deviation averages to 1°C and is even lower for high regeneration temperatures. Simulated temperature is higher

than reference data, which can be explained due to higher dehumidification in the simulation. This leads to higher latent heat flux and therefore to the increased outlet temperature.

Figure 13 shows air outlet humidity for different rotating speeds at constant process and regeneration air inlet conditions. For low speeds, the matrix remains a long time on process air side and dehumidification capacity is exhausted before the drying period ends. At increasing speeds and shorter time periods, air dehumidification is higher and reaches a maximum value (lowest outlet humidity). For higher speeds, the process is dominated by heat transfer, thus dehumidification rate sinks. From figure 13 follows, that optimal rotating speed should be $u \approx 0.3 - 0.5$ rpm for this inlet conditions.

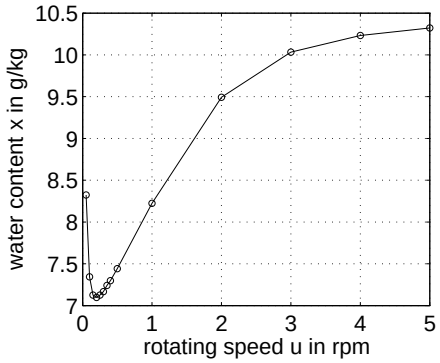

Figure 13: Air outlet water content for different desiccant wheel rotating speeds

As figure 14 shows, process air state changes change from adiabatic dehumidification ($h \approx$ const) to simultaneous mass and heat recovery from regeneration air at higher rotating speeds ($u \geq 5$ rpm). This effect is also known as enthalpy recovery and is used in practice in winter operation mode, to recover heat and humidity at different temperature and humidity levels between process and regeneration air. Hence, in winter, dry outside air can be humidified and heated by enthalpy recovery. Enthalpy recovery can be controlled by changing rotating speed.

4.3 Comparison to experimental data

Within the scope of a research project, experiments have been carried out at TUHH. Measured process and regeneration air states were used as input for the simulation. Figure 15 shows the inlet temperatures and simulated outlet water content and experimental results. Deviation between experiment and simulation ammounts approx. to 1 g/kg.

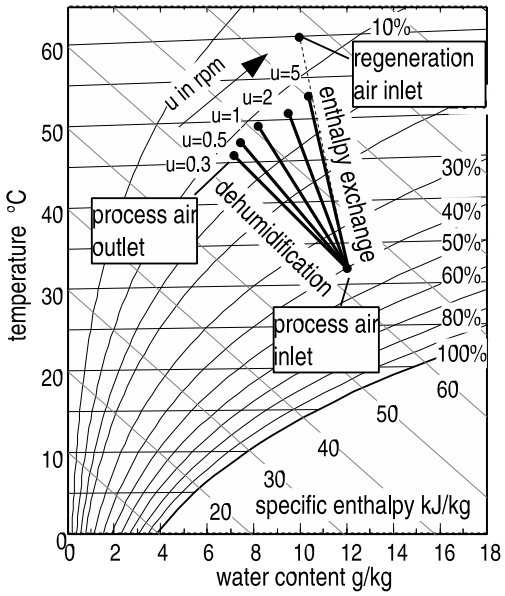

Figure 14: Air state changes for dehumidification and enthalpy exchange

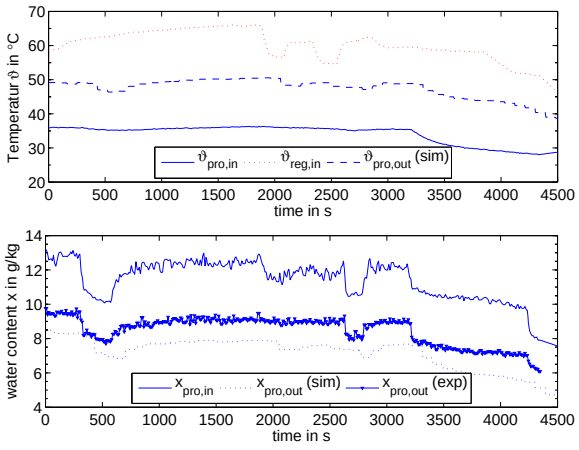

Figure 15: Simulation of LiCl desiccant wheel and comparison to experimental data

It has to be taken into account, that experimental results for outlet water content are calculated from relative humidity measurement and temperature. But at higher temperatures, e.g. for outlet process air, the accuracy for humidity measurement ($\pm$3% r.H.) results in an absolute error $\Delta x = 0.8$ g/kg. Simulation's deviation from experimental results is thus nearly between accuracy range. Furthermore, air flow measurement used as input for the simulation contains also approx. $5 - 10\%$ error. In addition, there is actually air carry over effect and air leakages which are not taken into account in the model. For high pressure differences between regeneration and process air, air flows directly from one side to the other making it difficult to deter-

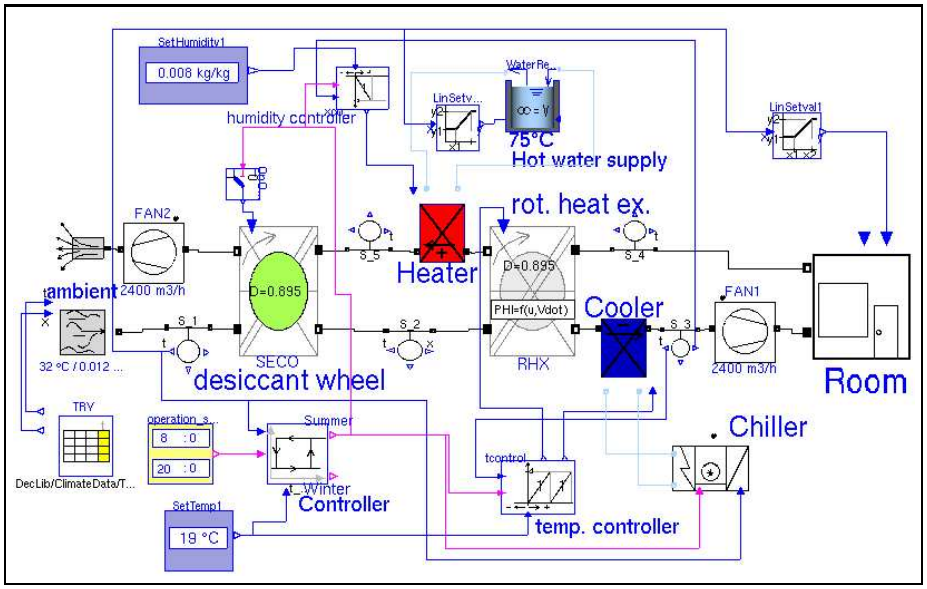

Figure 16: Desiccant assisted air conditioning plant

mine actual air state changes. Time delay in process outlet response for the simulation is an effect of mean value computation (90 s mean value). As stated above in section 3, tangential discretization should be used for changing inlet conditions.

4.4 Desiccant AC plant simulation

The presented Modelica models were used to simulate the performance of a desiccant air conditioning plant, see schematics in figure 16. The plant model includes models for reading climate data, heat exchanger (heater and cooler) and fan models as black box models, as well as models for temperature and humidity control.

Outside air first flows through the desiccant wheel, beeing subsequently pre-cooled using a rotating heat exchanger and finally cooled to supply air temperature. Air leaving the room passes first the rotating heat exchanger and is heated to regeneration air temperature in order to take the moisture out of the wheel. Temperature sequence controller regulates first the rotating speed of the rotating heat exchanger and secondly the cooling capacity of the cooler. Humidity control increases heat input in regeneration air heater if actual humidity higher than set value.

Figure 17 shows results for supply temperature and regeneration air temperature needed for dehumidification during a week in summer operation mode. Supply set value (19°C) can be mantained for the operation hours of the plant. As expected, regeneration air temperature varies with outside air humidity due to higher dehumidification load. For the simulation period, the calculated temperature of regeneration air remains under 60°C. This is advantageous, since low temperature heat sources can be used for the dehumidification process. Supply air humidity can be maintained within desired humidity level (8-9 g/kg). The resulting heating and cooling capacity can be seen in figure 18. The regeneration air heater has a heating capacity of 15 kW, whereas for cooling 7 kW are needed. Integrating capacity results in heating and cooling energy demand for the simulated period, e.g. 843 kWh heating, 434 kWh cooling demand.

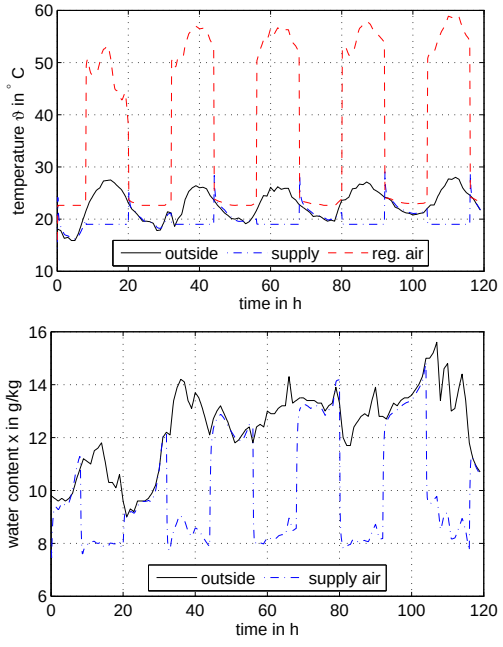

Figure 17: System simulation: temperatures and water content

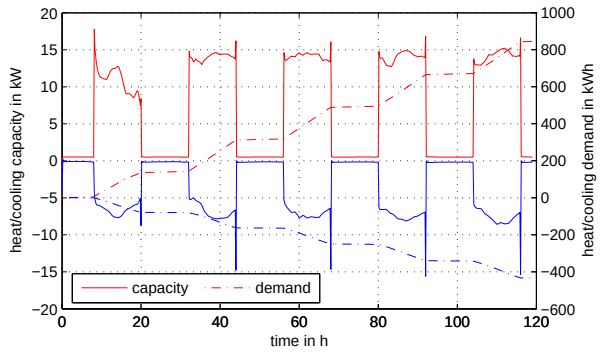

Figure 18: System simulation: heating/cooling capacity and demand

5 Conclusions

In this paper, a Modelica model for the simulation of air dehumidification by means of a desiccant wheel has been presented. The model is based on a finite volume approach for air and desiccant material. Heat and mass transfer are described by lumped convective coefficients. The model was tested for LiCl as desiccant, but can be used for other availabe desiccants, if equilibrium equations (sorption isotherm) are provided.
Transient simulation results are in good agreement with open literature. A comparison to manufacturer data was carried out. It turned out that available manufacturer data is not plausible for higher regeneration temperatures, whereas simulation returns a plausible behaviour according to desicant material properties.
Other components have also been modeled and used to calculate heating and cooling demand of a desiccant assisted air conditioning system.

References

[1] A. Campo, J.C. Morales, and A.E. Larreteguy. Pressure drop and heat transfer associated with flows moving laminarly in straight ducts of irregular, singly connected cross-sections. *Heat and Mass Transfer*, 32:193–197, 1997.

[2] W. Casas and G. Schmitz. Experiences with a gas driven, desiccant assisted air conditioning system with geothermal energy for an office building. *Energy and Buildings*, 37(5):493–501, 2005.

[3] W. Gutermuth. *Untersuchung der gekoppelten Wärme- und Stoffübertragung in Sorptionsregeneratoren*. PhD thesis, TH Darmstadt, 1980.

[4] Frank P. Incropera and David P. DeWitt. *Fundamentals of Heat and Mass Transfer*. John Wiley & Sons, 4 edition, 1996.

[5] E.F. Johnson and M.C. Molstad. Thermodynamic properties of aqueous lithium chloride solutions. *Journal of Physical Chemistry, American Chemical Society*, 55(2):257–281, 1951.

[6] I.L. MacLaine-cross and P.J. Banks. Coupled heat and mass transfer in regenerators – prediction using an analogy with heat transfer. *International Journal of Heat and Mass Transfer*, 15:1225–1242, 1972.

[7] B. Mathiprakasam and Z. Lavan. Performance predictions for adiabatic desiccant dehumidifiers using linear solutions. *Journal Solar Energy Engineering*, 102:73–79, 1980.

[8] J.L. Niu and L.Z. Zhang. Heat transfer and friction coefficients in corrugated ducts confined by sinusoidal arc curves. *Int. Journal of Heat and Mass Transfer*, 45:571–578, 2002.

[9] J.J. Rau, S.A. Klein, and J.W. Mitchell. Characteristics of lithium chloride in rotary heat and mass exchangers. *Int. Journal of Heat and Mass Transfer*, 34(11):2703–2713, 1991.

[10] K.W. Röben and J. Hupe. Zur kontinuierlichen gasentfeuchtung durch absorption und chemisorption. *Chemie-Technik*, 11(7):866–873, 1982.

[11] R.K. Shah and A.L. London. *Laminar Flow Forced Convection in Ducts*. Academic Press, New York, 1978.

[12] D.F. Sherony and C.W. Solbrig. Analytical investigation of heat or mass transfer and friction factors in a corrugated duct heat or mass exchanger. *Int. Journal of Heat and Mass Transfer*, 13:145–159, 1969.

[13] C.J. Simonson and Robert W. Besant. Heat and moisture transfer in desiccant coated rotary energy exhangers: Part i. numerical model. *ASHRAE International Journal of Heating, Ventilating, Air Conditioning and Refrigeration, HVAC& Research*, 3(4):325–350, 1997.

[14] W. Zheng and W.M. Worek. Numerical simulation of combined heat and mass transfer processes in a rotary dehumidifier. *Numerical Heat Transfer, Part A*, 23:221–232, 1993.